Variability of UVR Effects on Photosynthesis of Summer Phytoplankton Assemblages from a Tropical Coastal Area of the South China Sea[†]

Kunshan Gao*[1,2,3], Gang Li[1], E. Walter Helbling[‡1] and Virginia E. Villafañe[‡1]

[1]Marine Biology Institute, Shantou University, Shantou, Guangdong, China
[2]State Key Laboratory of Marine Environmental Science, Xiamen University, Xiamen, China
[3]State Key Laboratory of Freshwater Ecology and Biotechnology, Institute of Hydrobiology, Chinese Academy of Sciences, Wuhan, Hubei, China

ABSTRACT

From June to September 2005, we carried out experiments to determine the ultraviolet radiation (UVR) -induced photoinhibition of summer phytoplankton assemblages from a coastal site of the South China Sea. Variability in taxonomic composition was determined throughout the summer, with a peak chlorophyll *a* (chl *a*~20 μg chl *a* L^{-1}) dominated by the diatom *Skeletonema costatum* that was detected early in the study period; the rest of the time samples were characterized by monads and flagellates, with low chl *a* values (1–5 chl *a* μg L^{-1}). Surface water samples were placed in quartz tubes, inoculated with radiocarbon and exposed to solar radiation for 2–3 h to determine photosynthetic rates under three quality radiation treatments (*i.e.* PAB, 280–700 nm; PA, 320–700 nm and P, 400–700 nm) using different filters and under seven levels of ambient irradiance using neutral density screens (*P vs E* curves). UVR inhibition of samples exposed to maximum irradiance (*i.e.* at the surface) varied from −12.2% to 50%, while the daytime-integrated UVR-related photoinhibition in surface seawater varied from −62% to 7%. The effects of UVR on the photosynthetic parameters P^B_{max} and E_k were also variable, but UV-B accounted for most of the observed variability. During sunny days, photosynthesis of microplankton (> 20 μm) and piconanoplankton (< 20 μm) were significantly inhibited by UVR (mostly by UV-B). However, during cloudy days, while piconanoplankton cells were still inhibited by UVR, microplankton cells used UVR (mostly UV-A) as the source of energy for photosynthesis, resulting in higher carbon fixation in samples exposed to UVR than the ones exposed only to photosynthetically active radiation (PAR). Our results indicate that size structure and cloudiness clearly condition the overall impact of UVR on phytoplankton photosynthesis in this tropical site of South China. In addition, model predictions for this area considering only PAR for primary production might have underestimated carbon fixation due to UVR contribution.

INTRODUCTION

Phytoplankton cells are important primary producers that contribute for a substantial share of CO_2 fixation in marine ecosystems. In the water column, phytoplankton within the euphotic zone (1% of surface visible radiation) utilize solar energy to fix carbon and, ultimately, to produce organic matter. In this layer, however, cells are exposed not only to photosynthetically active radiation (PAR; 400–700 nm) but also to ultraviolet radiation (UVR; 280–400 nm), which can penetrate to considerable depths (1). While PAR is the most important waveband involved in the photosynthetic process, UVR is usually regarded as an important stressor for phytoplankton (2) as it can damage important cellular components such as the DNA molecule or proteins (2,3) or affect the physiological processes, *e.g.* photosynthesis and growth (4), nutrient uptake (5) or fatty acids composition (6). On the other hand, UVR (especially UV-A, 315–400 nm) has been found to enhance carbon fixation under relatively low solar irradiance levels (7,8) or fast mixing conditions (9) and allow photorepair of UVR-induced DNA damage (3).

Responses to UVR of phytoplankton organisms are variable: For example, when addressing photosynthetic inhibition, some organisms are rather resistant, as those generally found in tropical areas, whereas some others are comparatively more sensitive, such as those characteristic of polar areas (10). Additionally, studies have also demonstrated the size dependence of UVR responses, with photosynthesis in small cells being less inhibited than that in large cells (11); however, they are more sensitive when addressing DNA damage (3,11). Within a specific geographical location, UVR effects are varied as well, as observed in prebloom, bloom and postbloom phytoplankton assemblages from the Patagonia coast of Argentina (12,13). Furthermore, studies addressing the impact of UVR upon natural phytoplankton communities of Chesapeake Bay (14) have determined no significant interseasonal differences in the responses to UVR; however, a significant intraseasonal variability in sensitivity has been observed when species were exposed to similar artificial UVR conditions. This variability in responses occurs because sensitivity and acclimation capacity are species specific (15) and also because the presence and dominance of species usually vary throughout the seasonal succession. Finally, seasonal changes in the UVR climate or

produced by ozone depletion events (16) as well as in other abiotic factors such as nutrient availability, temperature (17,18) or mixing dynamics (9) may account for much of the observed variability in UVR responses of phytoplankton organisms.

The aim of this study was to determine the temporal variability of UVR effects on phytoplankton photosynthesis throughout the summer in a coastal site of the South China Sea. In addition, we studied the impact of UVR on two cell size fractions—piconanoplankton ($<20~\mu m$) and microplankton ($>20~\mu m$). The significance of this work lies in the following facts: On one hand, our data on phytoplankton primary productivity as affected by solar radiation are especially important for our study area as it sustains aquaculture and high standing stock of commercial fish and invertebrate species. On the other hand, this study provides new knowledge on the effects of solar UVR upon natural phytoplankton communities from the South China Sea, where relatively few field photo-biological studies have been performed (9,19).

MATERIALS AND METHODS

Radiation measurements. Incident solar radiation was continuously measured using a broadband filter radiometer (ELDONET, Real Time Computers, Inc., Germany). The instrument records irradiance in three wavebands: UV-B (280–315 nm), UV-A (315–400 nm) and PAR (400–700 nm). A diving radiometer (ELDONET, Real Time Computers, Inc.) with the same channels as above as well as temperature and depth sensors was used to determine the underwater radiation field.
Temperature and conductivity. Profiles of conductivity and temperature in the sampling site were obtained at 20 cm intervals with a sonde (YSI 600XL, Yellow Spring Instruments, Yellow Springs, OH).
Study area/sampling protocol. This study was carried out in coastal waters of the South China Sea (23°24′N, 117°07′E) during summer 2005. The experiments were conducted at the Marine Biological Station of Shantou University located in Nan'Ao Island (Fig. 1). The study site was visited every 10–15 days during the period from June 26 to September 27, 2005 (Julian days 176–269). Surface water samples were taken 500 m offshore at a site with about 10 m depth during early morning with an acid-cleaned (1 N HCl) polycarbonate carboy and returned to the laboratory (15 min away from the sampling site) where experiments were performed as described below.
Experimentation on UVR effects. To determine the effects of solar UVR upon phytoplankton photosynthetic rates, samples were placed in 30 mL quartz tubes and inoculated with labeled sodium
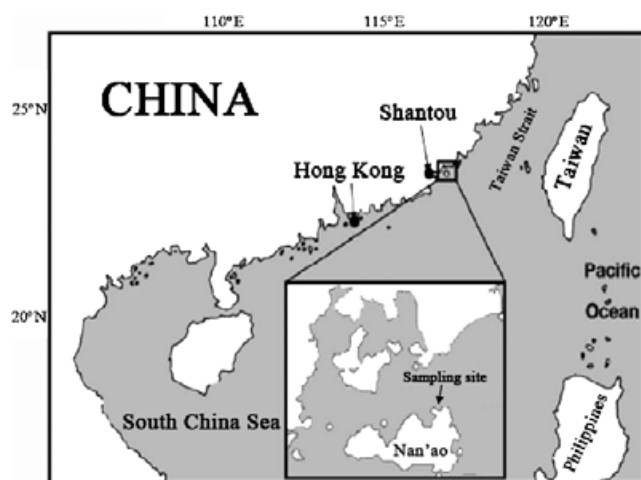

Figure 1. Map of the South China Sea, indicating the location of Nan'Ao Island, where experiments were carried out during the period June 26 to September 27, 2005 (Julian days 176–269).

bicarbonate (NaH^{14}CO$_3$, see below). Three radiation treatments were implemented (duplicates for each treatment except for Julian days 179, 195, 214 and 251, which were carried out in triplicate): (1) samples receiving PAR + UV-A + UV-B (280–700 nm, PAB treatment), unwrapped quartz tubes; (2) samples receiving PAR + UV-A (315–700 nm, PA treatment), tubes covered with Folex UV cutoff filter (Montagefolie, N°10155099, 50% transmission at 320 nm); and (3) samples receiving only PAR (400–700 nm, P treatment), tubes wrapped with Ultraphan UV Opak Digefra film (50% transmission at 395 nm). The spectra of these materials are published elsewhere (20). Additionally, two tubes were wrapped in aluminum foil to measure carbon fixation in darkness. The tubes containing the samples were put beneath the surface (1–2 cm) of a bath with running seawater to control temperature (27–30°C) and incubated under solar radiation for 2–3 h (centered on local noon). A total of 20 experiments were conducted during the study period.

UVR effects on *P vs E* parameters were determined by dispensing samples into 30 mL quartz tubes and inoculated with labeled sodium bicarbonate (see below) under three quality radiation treatments (as described above) and under seven levels of ambient irradiance (by covering the tubes with none or an increasing number of neutral density screens thus varying irradiance from 100 to <2%). A tray containing the tubes was then put in the water bath with running seawater for temperature control (27–30°C) and exposed to natural radiation for 2–3 h (incubations centered on local noon) as mentioned above. A total of six *P vs E* curves were obtained during the study period.

Additional experiments were conducted under cloudy and sunny conditions to determine carbon fixation under the three radiation treatments (as described above) in the piconanoplankton fraction ($<20~\mu m$ in effective diameter) as well as in the total population. The piconanoplankton fraction was obtained by gently filtering the samples through a 20 μm Nitex® mesh, before incubation with radiocarbon. Two experiments were carried out under sunny conditions (*i.e.* Julian days 195 and 214), whereas four were carried out under cloudy conditions (*i.e.* Julian days 179, 209, 251 and 264) during the study period.

Analyses and measurements. At the beginning of experiments, samples were taken to determine chlorophyll *a* (chl *a*) concentration and species composition; after incubation, samples were processed to determine photosynthetic rates. The analytical procedure for each determination/measurement was as follows:
Photosynthetic rates. Phytoplankton samples were inoculated with 0.1 mL–5 μCi (0.185 MBq) of labeled sodium bicarbonate (ICN Radiochemicals). After incubation, samples were filtered onto a Whatman GF/F glass fiber filter (25 mm); then, the filters were placed in 20 mL scintillation vials, exposed to HCl fumes overnight and dried (21). After this, scintillation cocktail (PerkinElmer®) was added to the vials and the samples were counted using a liquid scintillation counter (LS 6500 Beckman Coulter).
Chlorophyll a. Chlorophyll *a* concentration was determined by filtering 0.3–0.5 L of water sample onto a Whatman GF/F glass fiber filter (25 mm) followed by extraction with absolute methanol for 3 h at room temperature and subsequent determination of the optical density using a scanning spectrophotometer (Shimadzu model UV 2501-PC, Japan). chl *a* concentration was calculated using the equations of Porra (22). To determine chl *a* concentration in the piconanoplankton fraction, a subsample was prefiltered through a Nitex® mesh (20 μm) and the extraction of photosynthetic pigments was performed as described above.
Species composition analysis. Samples were fixed with buffered formalin (final concentration of 0.4% in the sample). The quantitative analysis of phytoplankton cells was carried out using an inverted microscope (Leica DM IL, Germany) after settling 10 mL of sample for 24 h (23).
Statistics. The parameters of the *P vs E* curves were obtained using the model of Eilers and Peeters (24) and fitting the data by iteration:

$$P^{B} = E/(aE^2 + bE + c),$$

where P^{B} is the production (μg C (μg chl *a*)$^{-1}$ h^{-1}), *E* is the irradiance (W m^{-2}) and *a*, *b* and *c* are the adjustment parameters. The initial slope (*i.e.* α), the maximum production rate (P^{B}_{max}) and the light saturation parameters (E_k) were expressed as a function of *a*, *b* and *c* parameters as follows:

$$E_k = (c/a)^{1/2}; \alpha = 1/c; P_{max}^B = 1/(b + 2(ac)^{1/2}).$$

The parameter "*a*" is considered the photoinhibition term but, according to modifications of Eilers and Peeters (24), it can also be interpreted as a function of the exposure time above E_k (25).

The daily primary production at the surface was estimated by integrating the predicted rate of photosynthesis over the daylight period:

$$\sum PP = \int_{t=sunrise}^{sunset} PAR(t)/(a \times PAR^2(t) + b \times PAR(t) + c) \times [chl\ a],$$

where $\sum PP$ represents the primary production; *a*, *b* and *c* are the adjustment parameters described above, whereas [chl *a*] represents the chl *a* concentration. Additionally, the ratio of UV-B:UV-A:PAR was assumed to remain the same as during the midday incubation period.

UVR-induced inhibition of photosynthetic carbon fixation or daily primary production was calculated as follows:

$$Inh(\%) = (P_{PAR} - P_{UVX})/P_{PAR} \times 100\%,$$

where Inh represents the UVR-induced inhibition, P_{PAR} and P_{UVX} the carbon fixation rates (or integrated primary production) under PAR alone or PAR + UVR treatments, respectively. UV-B–induced inhibition was calculated using the following formula:

$$Inh(\%) = (P_{UVA} - P_{UVR})/P_{PAR} \times 100\%,$$

where P_{UVA} is the PAR + UV-A and P_{UVR} is the PAR + UV-A + UV-B incubation (or predicted daily productivity).

Mean and half range were used to present the values in the figures for the experiments carried out with duplicate samples, whereas mean and standard deviations were used in the case of triplicate samples; standard errors of the *P* and *E* parameters and daily inhibition were derived using propagation of errors. One-way ANOVA (26) was used to determine the significant differences between the treatments for the results of the July 15 fractionation experiment (three replicate samples per treatment, confidence level = 0.05), while a two sample pairwise *t*-test was used to compare the photosynthetic parameters (*i.e.* P_{max}^B and E_k) among three treatments (*i.e.* PAB, PA and P) using a confidence level of 0.05.

RESULTS

Total ozone column concentration and daily doses of solar radiation for the study period—June 26 to September 27, 2005 (Julian days 176–269)—are shown in Fig. 2. Ozone column concentration over Shantou (data obtained from http://jwocky.gsfc.nasa.gov/) was variable, although there was a slight trend of decreasing values toward the end of the summer; maximum and minimum ozone concentrations were 297 and 259 Dobson Units, on days 203 and 222, respectively (Fig. 2a). Incident solar radiation (Fig. 2b–d) displayed a high variability because of differences in cloud cover throughout the study period. UV-B daily doses varied between 73.2 and 5.29 KJ m^{-2} (Fig. 2b), whereas UV-A varied between 2.37 and 0.19 MJ m^{-2} (Fig. 2c). PAR followed the same trend as UVR wavebands with daily doses ranging between 13.9 and 0.9 MJ m^{-2} (Fig. 2d). The ratio of UV-B to PAR during the study period varied between 0.63% and 0.45%, on days 233 and 251, respectively.

Physical and biological characteristics of the study area during summer 2005 are presented in Figs. 3 and 4. A typical vertical profile (Fig. 3) obtained on Julian day 176 showed changes in temperature, salinity and solar radiation with water depth. For the whole investigation period, the attenuation coefficients of PAR, UV-A and UV-B ranged between 0.58–0.78 m^{-1}, 1.31–1.53 m^{-1} and 2.01–2.73 m^{-1}, respectively. The
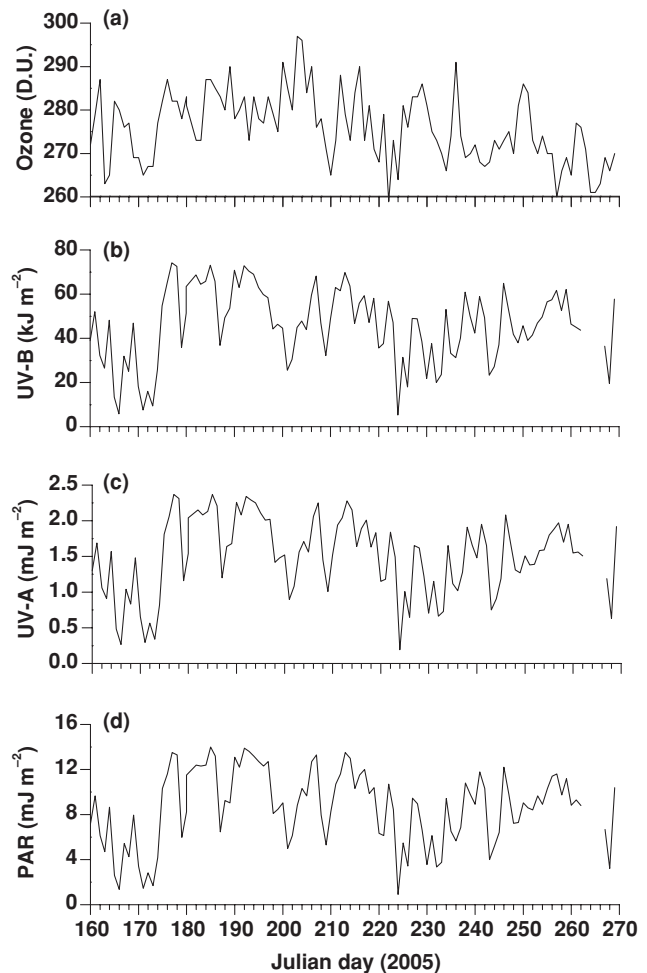

Figure 2. Atmospheric conditions for the period from June 15 to September 27, 2005 (Julian days 160–269). (a) Total ozone column concentrations (in Dobson Units, DU); (b) daily doses of UV-B, 280–315 nm (in KJ m^{-2}); (c) daily doses of UV-A, 315–400 nm (in MJ m^{-2}); and (d) daily doses of photosynthetically active radiation [PAR; 400–700 nm (in MJ m^{-2})]. No solar radiation data were collected during Julian days 263–266.

lower limit of the euphotic zone ranged from 6 to 8 m; 99% of UV-A was attenuated at depths of 3–3.5 m (1.7–2.3 m for UV-B), and depth of upper mixing layer ranged from 2 to 7 m. Temperature and salinity in surface waters varied greatly as well, with temperature ranging from 25.5°C to 28.2°C, and salinity from 21.8 to 32.5 (Fig. 4a). Particularly, the low salinity values determined on Julian day 181 were associated with a tropical storm on the Julian day 162 that brought heavy rains continuously over the study area. Biological characteristics were also variable, with phytoplankton biomass presenting a peak of ∼20 µg chl *a* L^{-1} during early summer (*i.e.* Julian day 179) and being relatively low (*i.e.* 1–5 chl *a* µg L^{-1}) throughout the rest of the study period (Fig. 4b). The peak of chl *a* was related to the presence of microplankton cells while during the rest of the time, piconanoplankton accounted for > 60% of the chl *a* allocation. The peak of high chl *a* values also had high cell concentrations (∼11 000 cells mL^{-1}) with the diatom *Skeletonema costatum* being the most abundant species; the diatoms *Asterionellopsis glacialis* and *Leptocylindrus*
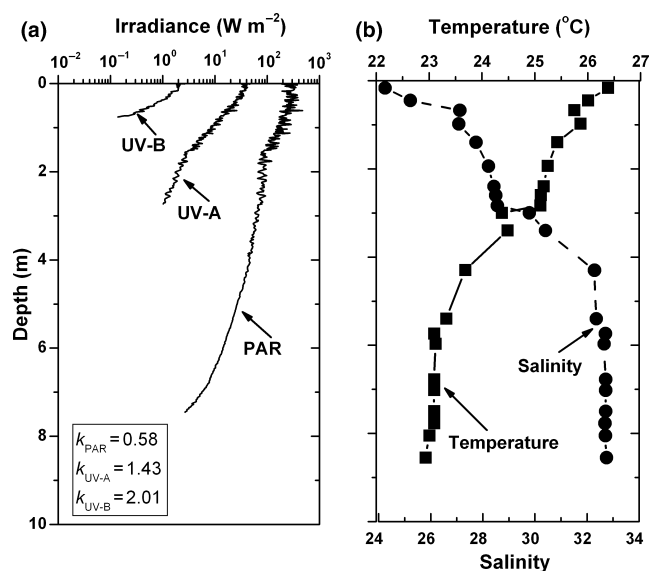
Figure 3. (a) Representative underwater radiation profiles of PAR (400–700 nm), UV-A (315–400 nm) and UV-B (280–315 nm) in W m^{-2}, with inset indicating the attenuation coefficients (k) in m^{-1} for these wavebands. (b) Vertical profiles of temperature (in °C, black squares) and salinity (black circles) in the water column. All the profiles were measured at sampling site on Julian day 176.

sp. were also numerically important during this period. On the other hand, the low biomass period was characterized by relatively low cell concentrations (300–3000 cells mL^{-1}) with monads and flagellates being the most abundant groups. The concentration of dinoflagellates was negligible throughout the study period. Carbon fixation by phytoplankton was also variable and ranged, in the P treatment, from a maximum value of 86 μg C L^{-1} h^{-1} (during the high chl *a* period) to a minimum of 8.5 μg C L^{-1} h^{-1} (Fig. 4c). Relatively high carbon fixation values were also found during the study period (*i.e.* on Julian days 208 and 248) and they were associated with a relative increase in large cells (Fig. 4b). Carbon fixation of samples in the PAB treatment was lower than that in the P treatment during most of the experiments, except in a few cases (*e.g.* Julian days 208, 209 and 251); carbon fixation in the PA treatment had intermediate values between those of the P and PAB treatments (data not shown). Finally, inhibition of carbon fixation due to UVR exposure varied from ∼50% (*i.e.* Julian day 195) to −12.2% (Julian day 209) thus indicating the use of UVR energy for photosynthesis (Fig. 4d).

The *P vs E* characteristics of natural phytoplankton assemblages are shown in Figs. 5 and 6. There were a range of responses but in general, all samples displayed little or no photoinhibition at PAR irradiances < 200 W m^{-2} (about 1000 μmol m^{-2} s^{-1}); at higher PAR irradiances though, photoinhibition was important in some samples, *e.g.* Julian days 195 and 228. The range of variability in *P vs E* parameters, as well as the impact of solar radiation on P^{B}_{max} and E_k is shown in Fig. 6. Maximum production rate (P^{B}_{max}) values (Fig. 6a) were relatively low (*i.e.* ∼4 μg C [μg chl *a*]$^{-1}$ h^{-1}) at the beginning of the sampling period, but they increased significantly (*i.e.* 14–16.8 μg C [μg chl *a*]$^{-1}$ h^{-1}) from Julian day 195 on. The impact of UVR on P^{B}_{max} was significant only in some samples—*e.g.* Julian day 252, with those under the PAB treatment being significantly
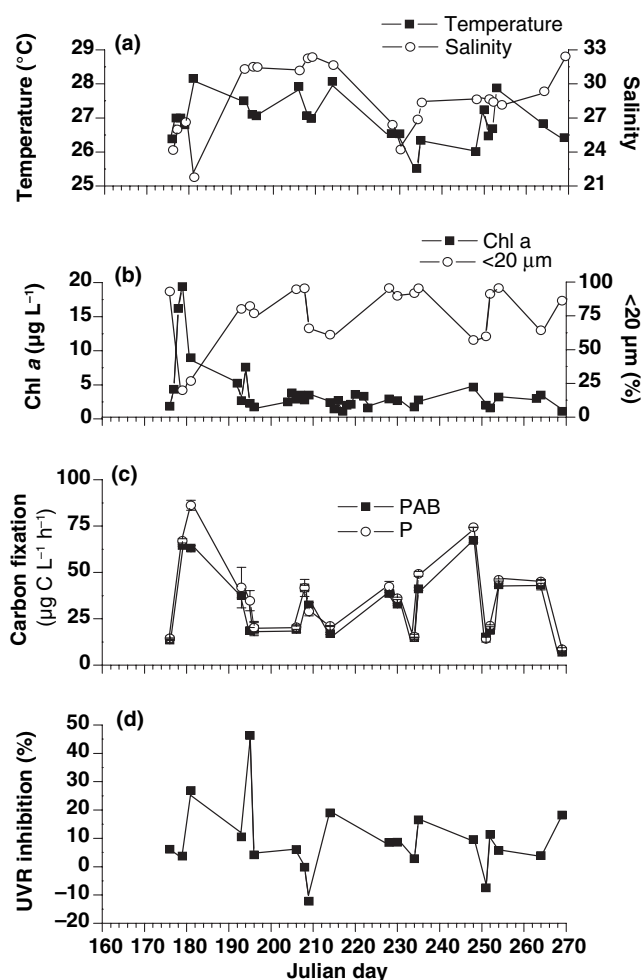

Figure 4. General physical and biological characteristics of the study area during Julian days 176–269, 2005. (a) Surface seawater temperature (in °C, black squares) and salinity (white circles); (b) chlorophyll *a* concentration (chl *a*; in μg L^{-1}, black squares) and percentage of chl *a* in the piconanoplankton fraction (< 20 μm, white circles); (c) average carbon fixation (in μg C L^{-1} h^{-1}) of phytoplankton assemblages exposed to PAB (280–700 nm, black squares) and P treatments (400–700 nm, white circles); (d) UVR inhibition (in %). Vertical bars on top of the symbols represent half of the range ($n = 2$ for each treatment) except Julian days 179, 195, 214 and 251 when standard deviation ($n = 3$ for each treatment) was applied.

different from those in the P treatment. The variations in the light saturation parameter E_k are shown in Fig. 6b. E_k was low at the beginning of summer (*i.e.* 27–45 W m^{-2}) and high later on (*i.e.* 100–115 W m^{-2}). As before, the UVR impact on E_k was variable, with UV-B accounting for bulk of the inhibition (*i.e.* Julian days 208, 228 and 252). Finally, the daily inhibition in surface seawater (calculated from data obtained from the *P vs E* curves) was also variable during the study period (Fig. 6c) but in general, there was a negative inhibition (*i.e.* the samples that received UVR fixed more carbon than those that received only PAR) reflecting the fact that phytoplankton was using UVR as the source of energy for photosynthesis.

The effects of solar UVR on different size fractions (piconanoplankton and microplankton) during representative sunny and cloudy days of the study period are shown in Figs. 7 and 8, respectively. During sunny days (*i.e.* maximum PAR
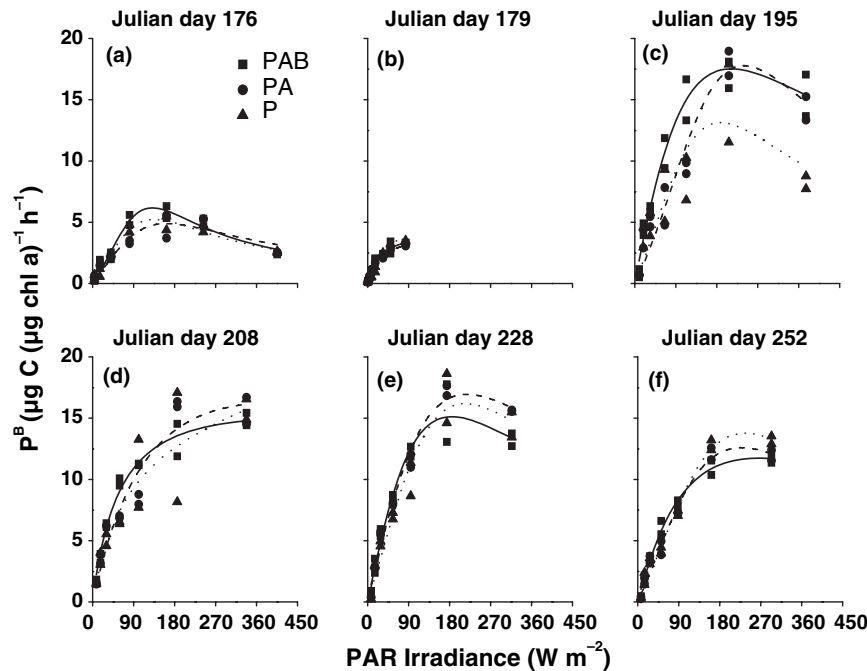
Figure 5. Phytoplankton P^B (in μg C [μg chl a]$^{-1}$ h^{-1}) as a function of the mean PAR irradiance (in W m^{-2}) to which samples from Nan'Ao were exposed. Black squares: Samples exposed to PAR + UV-A + UV-B (PAB, 280–700 nm); black circles: Samples exposed to PAR + UV-A (PA, 320–700 nm); black triangles: Samples exposed to PAR only (P, 400–700 nm). R^2 for the relationship of P^B and PAR ranged from 0.52 to 0.97 (n = 14). The experiments were carried out on: (a) June 26 (Julian day 176); (b) June 29 (Julian day 179); (c) July 15 (Julian day 195); (d) July 28 (Julian day 208); (e) August 17 (Julian day 228); and (f) September 10 (Julian day 252).

irradiance at local noon of 428.3 W m^{-2}, Fig. 7a), assimilation numbers in piconanoplankton and microplankton were similar in the PAB treatment ($\sim$5 μg C [μg chl a]$^{-1}$ h^{-1}). However, there were significant differences in assimilation numbers among size fractions in the PA and P treatments, with those in small cells being 51% and 54% lower than that in microplankton, respectively (Fig. 7b). The rate of carbon fixation (Fig. 7c), however, was significantly higher in small (6.02–10.25 μg C L^{-1} h^{-1}) than in large cells (1.63–6.68 μg C L^{-1} h^{-1}) in all radiation treatments, reflecting the higher proportion of small cells in the assemblages (i. e. $\sim$76.9% of the chl a). The relative UVR-induced photoinhibition (as compared with the P treatment) reached maximum values of 77% and 41% for microplankton and piconanoplankton communities, respectively, with UV-B accounting for most of the inhibition in both size fractions (Fig. 7d).

During cloudy days (*i.e.* maximum PAR irradiance at local noon of 302.3 W m^{-2}, Fig. 8a), assimilation numbers in piconanoplankton were lower than that in microplankton, except for the P treatment (Fig. 8b). Carbon fixation was higher in small than in large cells (Fig. 8c) however, in microplankton it was higher under full solar radiation (PAB treatment) than when cells received only visible radiation P treatment (Fig. 8c); therefore, microplankton displayed negative inhibition values as much as 95% (Fig. 8d). On the other hand, UVR-induced photoinhibition in piconanoplankton was positive, with values < 20% (Fig. 8d).

DISCUSSION

The geographical location of the study area in the tropical part of China, as well as the time frame for experimentation, had

provided a unique opportunity to evaluate the effects of solar radiation on natural phytoplankton assemblages exposed to high PAR and UVR levels. In the present study, we focused on one of the most noticeable effects caused by solar radiation—photoinhibition (*i.e.* the reduction of photosynthesis rates under high radiation levels), which occurs in most autotrophic organisms including phytoplankton (4). In the following paragraphs, we will discuss the main causes involved in the responses of phytoplankton observed during our experiments.

During the study period, the relatively high UV-B levels were associated with the lower ozone column concentrations over Nan'Ao (*i.e.* 260–290 Dobson Units, Fig. 2a) as compared with those characterizing high latitude sites (27). The daily doses of PAR and UV-A measured in our study area are comparable with those in coastal environments of Patagonia (28), where the combination of high irradiances and long day period results in high PAR and UVR daily doses (29). However, higher doses of UV-B were determined in our study site in Southern China. In addition, UV-B to PAR ratios during the incubation period ranged from 0.71% to 0.86% (UV-A/PAR, 15.5–17.8%), being higher than those at mid latitudes at the same time of the year (28). Low levels of UV-A and PAR are known to activate repairing processes for damage on DNA or proteins caused by UV-B (3,30). Therefore, UV-B/UV-A/PAR ratios are very important from an ecological point of view as they determine the balance between damage and repair in organisms (31).

During the study period, there was a clear peak of phytoplankton biomass ($\sim$20 μg chl a L^{-1}) dominated by relatively large cells, whereas the rest of the time (with chl a < 10 μg L^{-1}) the crop was characterized by piconanoplankton species (Fig. 4b). Even though the period of high chl a
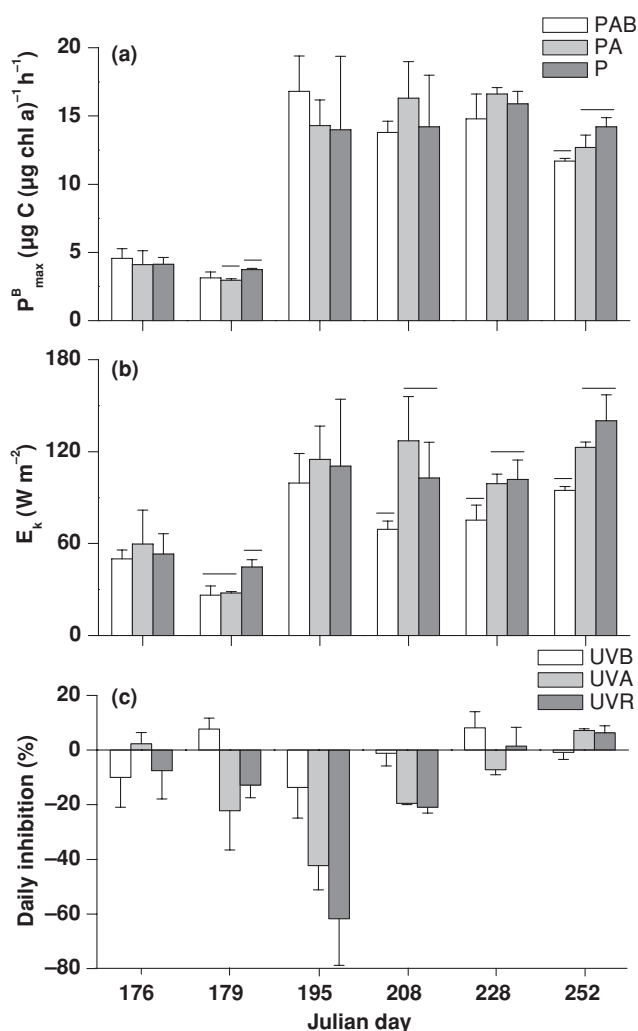
Figure 6. Mean photosynthetic parameters for the six experiments carried out with samples collected at Nan'Ao. (a) Mean P^B_{max} (in μg C $[\mu$g chl $a]^{-1}$ h^{-1}) and (b) mean E_k (in W m^{-2}). White bars: Samples exposed to PAR + UVR (PAB, 280–700 nm); Gray bars: Samples exposed to PAR + UV-A (PA, 320–700 nm); Black bars: Samples exposed to PAR only (P, 400–700 nm). (c). Daily photosynthetic inhibition (in %) in the surface seawater due to UV-B (white bars), UV-A (gray bars) and UVR (black bars). The vertical lines on top of the bars represent one standard error (calculated by propagation of errors, see Materials and Methods), whereas the horizontal lines represent significant differences between treatments for each fraction (P < 0.05).

concentration was associated with high carbon fixation, high photosynthetic rates were also observed at other times (Fig. 4c), which may be related to the different photoacclimation or cells composition (13). The temporal variations in phytoplankton taxonomic composition might have been related to changes in the physical characteristics of the water column (32) (*i.e.* stability) in turn associated with the meteorological conditions prevailing in this area, where heavy rains are common in the summer (data not shown) with concomitant changes in salinity (Fig. 4a). This, together with variations in surface temperature, affected the overall stability of the water column further. In addition, grazing pressure could be responsible for the observed changes in phytoplankton abundance (33).
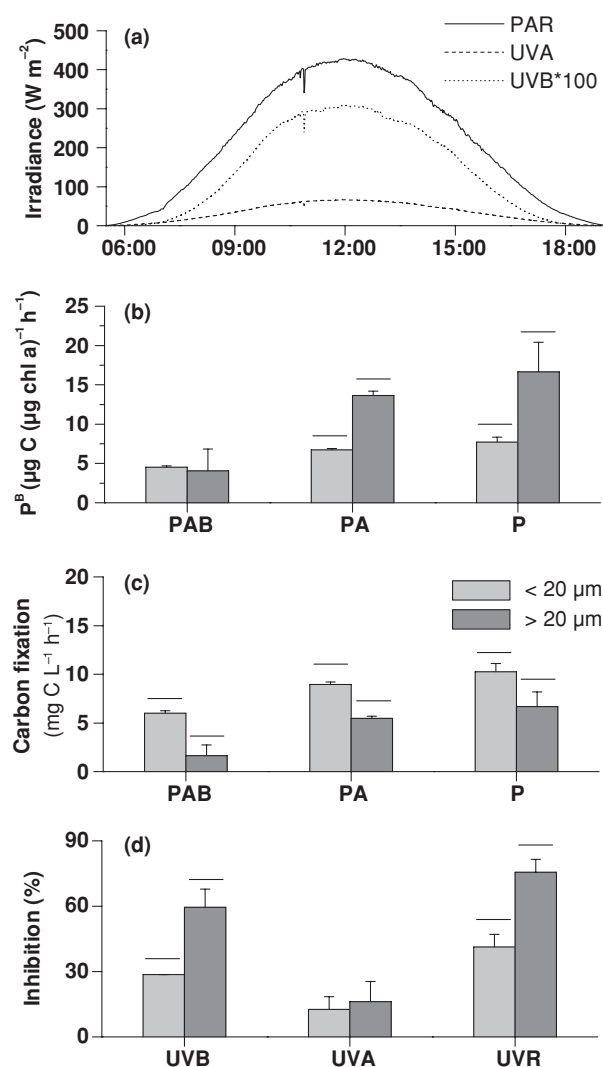

Figure 7. Effects of solar radiation on different phytoplankton fractions in a representative sunny day of the study period (July 15, Julian Day 195): (a) Incident PAR (400–700 nm, solid line), UV-A (315–400 nm, broken line) and UV-B (280–315 nm, dotted line), units are W m^{-2}; (b) P^B (in μg C $[\mu$g chl $a]^{-1}$ h^{-1}) of piconanoplankton (<20 μm, gray bars) and microplankton (>20 μm, black bars) exposed to PAB (280–700 nm), PA (320–700 nm) and P (400–700 nm) treatments; (c) carbon fixation (in μg C L^{-1} h^{-1}) of piconanoplankton (gray bars) and microplankton (black bars) exposed to PAB, PA and P treatments; (d) percentage inhibition due to UV-B, UV-A and UVR on piconanoplankton (gray bars) and microplankton cells (black bars). The vertical bars represent one standard deviation (n = 3 for each treatment), whereas the horizontal lines represent significant differences between treatments for each fraction (P < 0.05).

Cell size is one of the important factors influencing the phytoplankton distribution and community structure as it determines their metabolic and growth rates (34,35). In our nutrient rich coastal area (36), small cells accounted for the bulk of phytoplankton, with piconanoplankton contributing more than 60% of the phytoplankton biomass in terms of chl a concentration (Fig. 4b). Small cells showed less UVR-induced inhibition of photosynthetic carbon fixation than large cells during sunny days (Fig. 7d). Photosynthetic carbon fixation of small cells (<2 μm in effective diameter) was found to be less
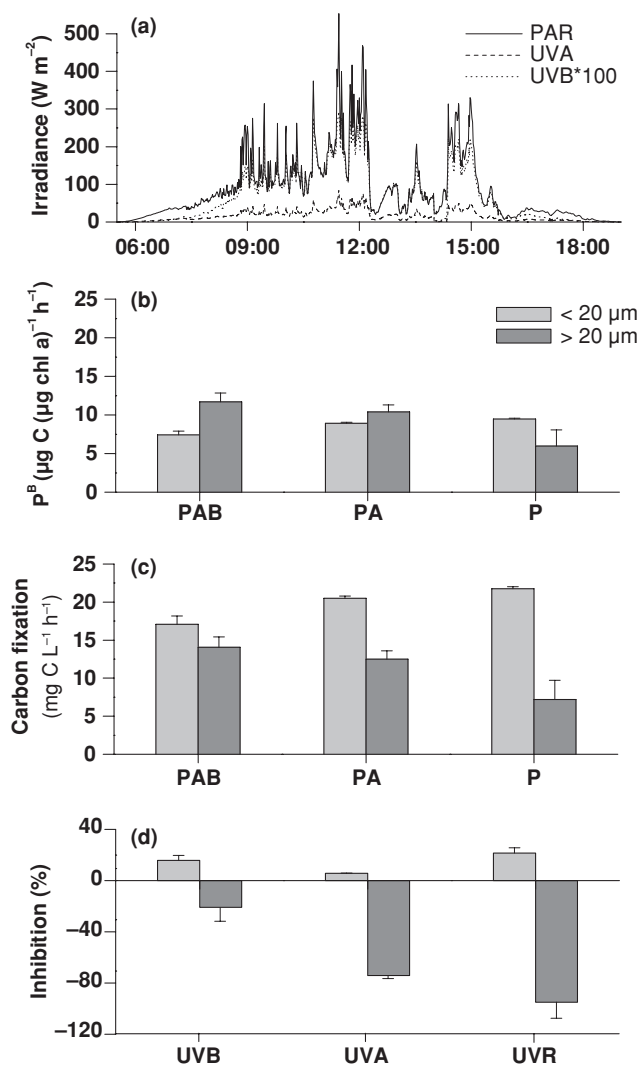
Figure 8. Effects of solar radiation on different phytoplankton fractions in a representative cloudy day of the study period (July 29, Julian Day 209): (a) Incident PAR (400–700 nm, solid line), UV-A (315–400 nm, broken line) and UV-B (280–315 nm, dotted line), units are W m^{-2}; (b) P^B (in μg C [μg chl a]$^{-1}$ h^{-1}) of piconanoplankton (<20 μm, gray bars) and microplankton (>20 μm, black bars) exposed to PAB (280–700 nm), PA (320–700 nm) and P (400–700 nm) treatments; (c) carbon fixation (in μg C L^{-1} h^{-1}) of piconanoplankton (gray bars) and microplankton (black bars) exposed to PAB, PA and P treatments; (d) percentage inhibition due to UV-B, UV-A and UVR on piconanoplankton (gray bars) and microplankton cells (black bars). The vertical bars represent half of the range (n = 2 for each treatment).

inhibited, though their DNA would be expected to be more damaged by UVR, compared with large cells (11,37). On cloudy days, however, large cells appeared to utilize UVR as the source of energy for photosynthesis and thus cells under the PAB treatment had higher carbon fixation than those under the P treatment (Fig 8c). Similar results have been found in other studies (8) and also at our study site (9) with the whole phytoplankton assemblages. In addition, it has been shown that microplankton cells are more resistant than nanoplankton (in terms of photosynthesis) if they synthesize UV-absorbing compounds (38), which are generally regarded as potential protectors against UVR stress (39). In our study, however, we

did not detect significant amounts of these compounds (data not shown), thus this strategy for protection against UVR stress would not be effective and instead, other alternative mechanisms such as photorepair (15,39) might be efficient.

Within a specific geographical region, phytoplankton assemblages with different light histories may reflect different photosynthetic characteristics (12,13). In Nan'Ao coastal waters, maximum production rates (P^B_{max}) varied from 3.0 to 16.8 μg C (μg chl a)$^{-1}$ h^{-1} throughout the study period (Fig. 6a) and photoinhibition was due to both PAR and UVR (Fig. 5). Light shocks after continuous cloudiness (Fig. 2b–d) or due to turbidity changes, caused by a tropical cyclone (*e.g.* on Julian day 162), which brought meroplankton up to the upper water layers, could be responsible for relatively "dark" acclimated cells and thus the high observed inhibition at some days (Fig. 4d). P^B_{max} and the light saturation parameter (E_k) increased slightly toward Julian day 195 (Fig. 6a,b) suggesting a photoacclimation with increasing solar radiation. However, during a period of relatively low solar radiation (Julian days 208–252, Fig. 2b–d), the UVR-induced inhibition on E_k reached values as high as 25% with the bulk being due to UV-B (Fig. 6b). Nevertheless, the photosynthetic apparent efficiency (α) in the presence of UVR was about 30% higher (data not shown) than that under PAR alone suggesting that UVR was utilized under low radiation levels. During the study period, although there was an important UVR-induced inhibition at high irradiances, when the daily photosynthetic production was integrated for surface seawater and compared among the treatments with or without UVR, the total effect resulted negative in most cases (*i.e.* enhancement of photosynthesis) suggesting that UV-A could add to the phytoplankton primary production in natural assemblages of the South China Sea (Fig. 6c). Moreover, based on our radiation data (Fig. 2b–d), we determined that there were 45 days during the whole summer period with PAR daily dose less than 8.92 MJ m^{-2} that can be defined as "cloudy," *i.e.* about half of the summer the irradiance conditions were similar to those represented in Fig. 8 with UVR adding significantly to the productivity of this area. Our results clearly contrast with those obtained in polar areas where UVR-induced inhibition of integrated primary production was reported to be about 20% each for UV-A and UV-B (40). Even though tropical environments have been considered to be acclimated to high levels of solar radiation, our study indicates that, in addition, phytoplankton can use UVR in the water column.

REFERENCES

1. Hargreaves, B. R. (2003) Water column optics and penetration of UVR. In *UV Effects in Aquatic Organisms and Ecosystems* (Edited by E. W. Helbling and H. E. Zagarese), pp. 59–105. The Royal Society of Chemistry, Cambridge.

2. Häder, D. P. (2003) Effects of solar ultraviolet radiation on aquatic primary producers. In *Handbook of Photochemistry and Photobiology* (Edited by H. S. Nalwa), pp. 329–352. American Scientific Publishers, Stevenson Ranch, California.

3. Buma, A. G. J., P. Boelen and W. H. Jeffrey (2003) UVR-induced DNA damage in aquatic organisms. In *UV Effects in Aquatic Organisms and Ecosystems* (Edited by E. W. Helbling and H. E. Zagarese), pp. 291–327. The Royal Society of Chemistry, Cambridge.

4. Villafañe, V. E., K. Sundbäck, F. L. Figueroa and E. W. Helbling (2003) Photosynthesis in the aquatic environment as affected by UVR. In *UV Effects in Aquatic Organisms and Ecosystems* (Edited by E. W. Helbling and H. E. Zagarese), pp. 357–397. The Royal Society of Chemistry, Cambridge.

5. Fauchot, J., M. Gosselin, M. Levasseur, B. Mostajir, C. Belzile, S. Demers, S. Roy and P. Z. Villegas (2000) Influence of UV-B radiation on nitrogen utilization by a natural assemblage of phytoplankton. *J. Phycol.* **36**, 484–496.

6. Goes, J. I., N. Handa, S. Taguchi and T. Hama (1994) Effect of UV-B radiation on the fatty acid composition of the marine phytoplankter *Tetraselmis sp.*: Relationship to cellular pigments. *Mar. Ecol. Prog. Ser.* **114**, 259–274.

7. Nilawati, J., B. M. Greenberg and R. E. H. Smith (1997) Influence of ultraviolet radiation on growth and photosynthesis of two cold ocean diatoms. *J. Phycol.* **33**, 215–224.

8. Barbieri, E. S., V. E. Villafañe and E. W. Helbling (2002) Experimental assessment of UV effects upon temperate marine phytoplankton when exposed to variable radiation regimes. *Limnol. Oceanogr.* **47**, 1648–1655.

9. Helbling, E. W., K. Gao, R. J. Goncalves, H. Wu and V. E. Villafañe (2003) Utilization of solar UV radiation by coastal phytoplankton assemblages off SE China when exposed to fast mixing. *Mar. Ecol. Prog. Ser.* **259**, 59–66.

10. Helbling, E. W., V. E. Villafañe, M. E. Ferrario and O. Holm-Hansen (1992) Impact of natural ultraviolet radiation on rates of photosynthesis and on specific marine phytoplankton species. *Mar. Ecol. Prog. Ser.* **80**, 89–100.

11. Helbling, E. W., A. G. J. Buma, M. K. de Boer and V. E. Villafañe (2001) *In situ* impact of solar ultraviolet radiation on photosynthesis and DNA in temperate marine phytoplankton. *Mar. Ecol. Prog. Ser.* **211**, 43–49.

12. Villafañe, V. E., E. S. Barbieri and E. W. Helbling (2004a) Annual patterns of ultraviolet radiation effects on temperate marine phytoplankton off Patagonia, Argentina. *J. Plankton Res.* **26**, 167–174.

13. Villafañe, V. E., M. A. Marcoval and E. W. Helbling (2004b) Photosynthesis versus irradiance characteristics in phytoplankton assemblages off Patagonia (Argentina): Temporal variability and solar UVR effects. *Mar. Ecol. Prog. Ser.* **284**, 23–34.

14. Banaszak, A. T. and P. J. Neale (2001) Ultraviolet radiation sensitivity of photosynthesis in phytoplankton from an estuarine environment. *Limnol. Oceanogr.* **46**, 592–603.

15. Roy, S. (2000) Strategies for the minimisation of UV-induced damage. In *The Effects of UV Radiation in the Marine Environment* (Edited by S. de Mora, S. Demers and M. Vernet), pp. 177–205. Cambridge University Press, Cambridge.

16. Blumthaler, M. and A. R. Webb (2003) UVR climatology. In *UV Effects in Aquatic Organisms and Ecosystems* (Edited by E. W. Helbling and H. E. Zagarese), pp. 21–58. The Royal Society of Chemistry, Cambridge.

17. Lesser, M. P. (1996) Elevated temperatures and ultraviolet radiation cause oxidative stress and inhibit photosynthesis in symbiotic dinoflagellates. *Limnol. Oceanogr.* **41**, 271–283.

18. Litchman, E., P. J. Neale and A. T. Banaszak (2002) Increased sensitivity to ultraviolet radiation in nitrogen-limited dinoflagellates: Photoprotection and repair. *Limnol. Oceanogr.* **47**, 86–94.

19. Gao, K., Y. Wu, G. Li, H. Wu, V. E. Villafañe and E. W. Helbling (2007) Solar UV radiation drives CO_2 fixation in marine phytoplankton: A double-edged sword. *Plant Physiol.* **144**, 54–59.

20. Figueroa, F. L., S. Salles, J. Aguilera, C. Jiménez, J. Mercado, B. Viñegla, A. Flores-Moya and M. Altamirano (1997) Effects of solar radiation on photoinhibition and pigmentation in the red alga *Porphyra leucosticta*. *Mar. Ecol. Prog. Ser.* **151**, 81–90.

21. Holm-Hansen, O. and E. W. Helbling (1995) Técnicas para la medición de la productividad primaria en el fitoplancton. In *Manual de Métodos Ficológicos* (Edited by K. Alveal, M. E. Ferrario, E. C. Oliveira and E. Sar), pp. 329–350. Universidad de Concepción, Concepción, Chile.

22. Porra, R. J. (2002) The chequered history of the development and use of simultaneous equations for the accurate determination of chlorophylls *a* and *b*. *Photosynth. Res.* **73**, 149–156.

23. Villafañe, V. E. and F. M. H. Reid (1995) Métodos de microscopía para la cuantificación del fitoplancton. In *Manual de Métodos Ficológicos* (Edited by K. Alveal, M. E. Ferrario, E. C. Oliveira and E. Sar), pp. 169–185. Universidad de Concepción, Concepción, Chile.

24. Eilers, P. H. C. and J. C. H. Peeters (1988) A model for the relationship between light intensity and the rate of photosynthesis in phytoplankton. *Ecol. Model.* **42**, 199–215.

25. Macedo, M. F., P. Duarte and J. G. Ferreira (2002) The influence of incubation periods on photosynthesis-irradiance curves. *J. Exp. Mar. Biol. Ecol.* **274**, 101–120.

26. Zar, J. H. (1984) *Biostatistical Analysis*, 2nd edn. Prentice Hall, Englewood Cliffs, NJ.

27. Madronich, S. (1993) The atmosphere and UV-B radiation at ground level. In *Environmental UV photobiology* (Edited by A. R. Young, L. O. Bjorn, J. Moan and W. Nultsch), pp. 1–39. Plenum Press, New York.

28. Helbling, E. W., E. S. Barbieri, M. A. Marcoval, R. J. Gonçalves and V. E. Villafañe (2005) Impact of solar ultraviolet radiation on marine phytoplankton of Patagonia, Argentina. *Photochem. Photobiol.* **81**, 807–818.

29. Orce, V. L. and E. W. Helbling (1997) Latitudinal UVR-PAR measurements in Argentina: Extent of the "ozone hole." *Glob. Planet Change* **15**, 113–121.

30. Sancar, A. and G. B. Sancar (1988) DNA repair enzymes. *Annu. Rev. Biochem.* **57**, 29–67.

31. Karentz, D. (1994) Ultraviolet tolerance mechanisms in Antarctic marine organisms. In *Ultraviolet Radiation and Biological Research in Antarctica* (Edited by C. S. Weiler and P. A. Penhale), pp. 93–110. American Geophysical Union, Washington, DC.

32. Sverdrup, H. U. (1953) On conditions for the vernal blooming of phytoplankton. *J. Cons. Perm. Int. Explor. Mer.* **18**, 287–295.

33. Alpine, A. E. and J. E. Cloern (1992) Trophic interactions and direct physical effects control phytoplankton biomass and production in an estuary. *Limnol. Oceanogr.* **37**, 946–955.

34. Raven, J. A. and J. E. Kübler (2002) New light on the scaling of metabolic rate with the size of algae. *J. Phycol.* **38**, 11–16.

35. Raven, J. A. (1998) Small is beautiful: The picophytoplankton. *Funct. Ecol.* **12**, 503–513.

36. Cai, W. J., M. H. Dai, Y. Wang, W. Zhai, T. Huang, S. Chen, F. Zhang and Z. Wang (2004) The biogeochemistry of inorganic carbon and nutrients in Pearl River estuary and the adjacent Northern South China Sea. *Cont. Shelf Res.* **24**, 1301–1319.

37. Boelen, P., M. K. de Boer, G. W. Kraay, M. J. W. Veldhuis and A. G. J. Buma (2000) UVBR-induced DNA damage in natural marine picoplankton assemblages in the tropical Atlantic Ocean. *Mar. Ecol. Prog. Ser.* **193**, 1–9.

38. Helbling, E. W., B. E. Chalker, W. C. Dunlap, O. Holm-Hansen and V. E. Villafañe (1996) Photoacclimation of Antarctic marine diatoms to solar ultraviolet radiation. *J. Exp. Mar. Biol. Ecol.* **204**, 85–101.

39. Banaszak, A. T. (2003) Photoprotective physiological and biochemical responses of aquatic organisms. In *UV Effects in Aquatic Organisms and Ecosystems* (Edited by E. W. Helbling and H. E. Zagarese), pp. 329–356. The Royal Society of Chemistry, Cambridge.

40. Helbling, E. W. and V. E. Villafañe (2002) UVR effects on phytoplankton primary production: A comparison between Arctic and Antarctic marine ecosystems. In *UV Radiation and Arctic Ecosystems* (Edited by D. Hessen), pp. 203–226. Springer-Verlag, Berlin Heidelberg.